

Chapter 11

Involvement of Manganese in Photosynthetic Water Oxidation

Gary W. Brudvig

Department of Chemistry, Yale University, New Haven, CT 06511

A multinuclear Mn complex functions in photosystem II to accumulate oxidizing equivalents and also to bind water and catalyze its four-electron oxidation. The Mn complex can exist in five oxidation states called S_i states ($i = 0-4$). Electron paramagnetic resonance (EPR), Mn K-edge X-ray absorption, and ultraviolet-absorption spectroscopies have been applied to study the structure and function of the Mn complex. The application of these methods to probe the Mn complex in photosystem II is briefly reviewed. Considering the results of both the X-ray absorption and EPR studies, a distortion of an oxo-bridged "cubane"-like Mn tetramer seems to best account for the arrangement of Mn ions in the S_2 state. Based on the known properties of the Mn complex in photosystem II and the coordination chemistry of Mn, structures were proposed for the five intermediate oxidation states of the Mn complex; these structures were incorporated into a molecular mechanism for the formation of an O-O bond and the displacement of O_2 from the S_4 state (Brudvig, G.W. and Crabtree, R.H. *Proc. Natl. Acad. Sci. USA* 1986, 83, 4586-88). This mechanism and the structure of the Mn complex are considered in light of recent studies of the Mn complex in photosystem II.

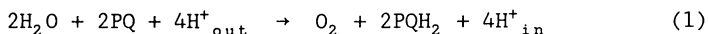
Although Mn occurs widely in biological systems, only a small number of enzymes have been identified that utilize oxidation states of Mn higher than +2. These redox-active Mn enzymes include the Mn superoxide dismutase, which is the only Mn enzyme in this group for which an X-ray crystal structure is available (1), the Mn-containing pseudocatalase (2), and photosystem II (for reviews see 3-6). Photosystem II is unique among this group of enzymes in that other transition metals have not been found to function in place of Mn, whereas alternate naturally-occurring forms of superoxide dismutase and catalase exist which contain Fe instead of Mn.

The function of photosystem II is to oxidize water and reduce

0097-6156/88/0372-0221\$06.00/0

• 1988 American Chemical Society

plastoquinone (PQ). In addition, photosystem II generates a pH gradient across the thylakoid membrane by producing and consuming protons on opposite sides of the membrane. The overall reaction, which requires four light-induced charge separations in the photosystem II reaction center, is:



where in and out refer to the inside and outside of the thylakoid vesicle, respectively.

Mn was first shown to play an important role in photosynthetic O_2 evolution by nutritional studies of algae (7). The stoichiometry of Mn in photosystem II was determined by quantitating Mn released from thylakoid membranes by various treatments (8). These experiments established that Mn is specifically required for water oxidation and that four Mn ions per photosystem II are required for optimal rates of O_2 evolution (9). More recently, photosystem II preparations with high rates of O_2 evolution have been isolated from a variety of sources (for a review see 10). The isolation of an O_2 -evolving photosystem II has proved to be a major step forward in both the biochemical and spectroscopic characterization of the O_2 -evolving system. These preparations contain four Mn ions per photosystem II (11), thus confirming that four Mn ions are functionally associated with each O_2 -evolving center.

Photooxidation of the Manganese Complex

To account for the periodicity of four in the yield of O_2 in a series of flashes (12-13), Kok and coworkers (14) proposed that photosystem II cycles through five states during flash illumination. These intermediate oxidation states are referred to as S_i states ($i = 0-4$) with the subscript denoting the number of oxidizing equivalents accumulated. The sequential advancement of the S states occurs via the light-induced charge separation in photosystem II.

A large body of evidence now supports the basic model put forward by Kok and coworkers (3-6,15). The S_4 state rapidly releases a molecule of O_2 and regenerates the S_0 state. The S_2 and S_3 states are unstable and are reduced in the dark to the S_1 state with half-times on the order of one minute at room temperature. Further, the S_0 state is oxidized in the dark to the S_1 state with a half-time on the order of ten minutes at room temperature (16-17). Hence, samples that are incubated in the dark for more than thirty minutes at room temperature contain only the S_1 state. In contrast, continuously illuminated samples contain equal fractions of states S_0 through S_3 which decay within a few minutes in the dark at room temperature to a mixture of S_0 and S_1 in a 1:3 ratio.

The question of the molecular basis for the S states has existed since the original proposal by Kok and coworkers. As first formulated, the S state designation referred to the oxidation state of the O_2 -evolving center which could, in principle, include all of photosystem II and its associated components. Indeed, there are a number of redox-active components on the electron-donor side of photosystem II in addition to the Mn complex, such as the tyrosine radical that gives rise to EPR signal II_s , and cytochrome b_{559} .

However, a change in the oxidation state of these species does not alter either the period-four oscillation of O_2 yields in a series of flashes, provided that the flashes are sufficiently closely spaced (16), or the EPR spectral properties of the S_2 state (18). Moreover, EPR (17-31) and X-ray absorption (32-38) studies have shown that Mn is oxidized in the S_1 to S_2 transition. Hence, it appears that the S states should be interpreted in terms of distinct intermediate oxidation states of the Mn complex (see below).

EPR Studies of the Manganese Complex

In general, one expects to observe an EPR signal from a transition metal complex whenever the complex possesses an odd number of unpaired electrons. If the complex possesses an even number of unpaired electrons, then spin-spin interactions may give rise to large zero-field splittings of the spin levels which will prevent the observation of EPR signals with conventional EPR instrumentation. Because each S-state transition involves the removal of one electron from the O_2 -evolving center, one predicts that alternate S states will have an odd number of unpaired electrons. These alternate S states should, in principle, be detectable by EPR spectroscopy. Indeed, the S_2 state exhibits a multiline EPR signal (Figure 1) from a multinuclear Mn complex (19). The S_2 -state multiline EPR signal was one of the first direct probes of the Mn complex in photosystem II and much of the information on the structure and function of the Mn complex has come from analyses of the S_2 -state EPR signals (17-31). However, a major limitation to the use of EPR spectroscopy to study the Mn complex is that measurements have been restricted to the S_2 state. Based on the argument that EPR signals are expected from alternate S states, one predicts that the S_0 state is a good candidate for detection by EPR spectroscopy. Nonetheless, an EPR signal has not yet been detected from the S_0 state.

Two distinct EPR signals have been observed from the S_2 state (Figure 1). The first is the multiline EPR signal centered at about $g = 2.0$. This EPR signal arises from an $S = 1/2$ state of a mixed-valence multinuclear Mn complex; the numerous hyperfine lines arise from the coupling of the unpaired electron to the nuclear spins of several Mn ions (each Mn ion has $I = 5/2$). The second EPR signal from the S_2 state exhibits a turning point at $g = 4.1$. The $g = 4.1$ EPR signal is generated by illumination of photosystem II membranes at 130 K, but is unstable and is converted into the multiline EPR signal upon warming to 200 K (18,22). However, the $g = 4.1$ EPR signal can be stabilized by the addition of various exogenous molecules including amines (29), fluoride (22), and sucrose (25).

Two interpretations of the identity of the species that gives rise to the S_2 -state multiline and $g = 4.1$ EPR signals have been proposed (24-26). Both EPR signals are proposed to arise from Mn centers. The difference in interpretations concerns the number of Mn ions involved in each paramagnetic species.

One view is that three distinct Mn centers function in the water oxidation process: two mononuclear Mn centers and a binuclear Mn center (26). It was proposed (26) that the binuclear center gives rise to the multiline EPR signal, whereas, one of the

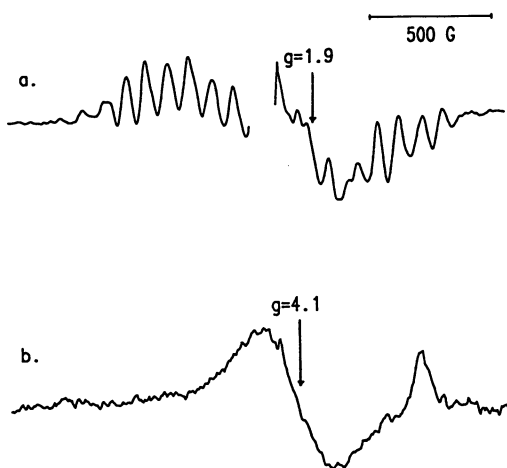


Figure 1: S_2 state EPR spectra: a) multiline EPR signal produced by illumination at 200 K; b) $g = 4.1$ EPR signal produced by illumination at 130 K. Experimental conditions are as in (24).

mononuclear Mn ions gives rise to the $g = 4.1$ EPR signal. In order to explain the stabilization of the $g = 4.1$ EPR signal by exogenous molecules, Hansson et al. (26) proposed that the $g = 4.1$ EPR signal arises from a mononuclear Mn(IV) in redox equilibrium with a binuclear Mn species. Hence, in the S_2 state, it was proposed that either the mononuclear Mn is oxidized to Mn(IV) and gives a $g = 4.1$ EPR signal or the binuclear Mn center is oxidized to Mn(III)-Mn(IV) and gives a multiline EPR signal. The reduction potentials of these two species must be comparable in the cases when the $g = 4.1$ EPR signal is stabilized. In this model, a further oxidation of the system to the S_3 state should leave both the binuclear and mononuclear centers oxidized. However, no EPR signal is observed from the Mn complex in the S_3 state which, in this model, requires that the $g = 4.1$ and multiline EPR signal species are magnetically coupled in the S_3 state. Hence, the redox equilibrium model requires that these two Mn species must be very close together.

The alternate proposal is that both the multiline and $g = 4.1$ EPR signals arise from the same tetranuclear Mn complex (18,24-25). The conversion of the $g = 4.1$ EPR signal into the multiline EPR signal upon incubation at 200 K in the dark can then be explained by a temperature-dependent structural change in the Mn site upon formation of the S_2 state, which alters the exchange couplings between the Mn ions (24). Generation of the S_2 state at 130 K may not allow such a rearrangement to occur rapidly and, hence, the $g = 4.1$ EPR signal could be viewed as an EPR signal arising from an S_1 -state conformation that is in the S_2 state. The structural difference between the " $g = 4.1$ " and "multiline" conformations need not be large; the conversion of the $g = 4.1$ EPR signal into the multiline EPR signal can be understood as a small rearrangement of the Mn complex into its preferred conformation in the higher oxidation state. Stabilization of the $g = 4.1$ EPR signal by exogenous molecules is explained in this model by stabilization of the " $g = 4.1$ " conformation.

These two models may not be significantly different. The main difference between them is the magnitude of the magnetic coupling proposed to exist between the four Mn ions in the S_2 state. However, the different Mn centers must be very close together in order to account for the absence of an EPR signal from the S_3 state.

The S_2 -state EPR signals have also been used to probe the coordination of exogenous ligands to the Mn complex (27-31). Ammonia, but not more bulky amines, dramatically alters the lineshape of the S_2 -state multiline EPR signal, indicating that ammonia binds directly to Mn in the S_2 state (28). The binding of ammonia to the Mn complex has been proposed to be a nucleophilic addition reaction and to model the binding of substrate water (27-29). Also, ^{17}O -labeled water slightly broadens the S_2 -state multiline EPR signal (30). The broadening of the S_2 -state multiline EPR signal in the presence of ^{17}O -labeled water under the conditions of these experiments indicates that exchangeable water is a ligand to Mn in the S_1 state. One can envision that water coordinates to the Mn site either as the substrate or in the form of a structural oxo-bridge. (The mode of binding may be equivalent in these two cases; the distinction can be made on the basis of the species that gives rise to O_2). Several studies, however, indicate that the substrate water is not bound to the Mn site in

the S_2 state (for a discussion see 27). By measuring the effect of ^{17}O -labeled water on the S_2 -state multiline EPR signal following incubation with a specific S state, one may be able to make a distinction between substrate water, which appears to bind to the Mn complex in one of the higher S states, and structural oxo-bridges between the Mn ions, which may be exchangeable but remain bound throughout the S -state cycle. ^{17}O -labeled water also broadens the altered S_2 -state multiline EPR signal formed in the presence of ammonia (31). One interpretation of this result is that the Mn complex in the ammonia-bound derivative of photosystem II contains exchangeable oxo-bridges between Mn ions that are not displaced by ammonia in the S_2 state.

X-ray Absorption Studies of the Manganese Complex

The oxidation states and ligation of Mn in photosystem II have been probed by X-ray absorption edge and extended X-ray absorption edge fine structure (EXAFS) measurements (32-38). EXAFS analyses have been done for Mn in the S_1 state present in dark-adapted thylakoid membranes (33,37) and in dark-adapted photosystem II membranes (35). These studies indicate that each Mn ion is probably six coordinate and ligated to oxygen and/or nitrogen ligands. Each Mn ion also sees 0.77 (35) or 2 - 3 (37) neighboring Mn ions at a distance of 2.7 Å. The EXAFS data for the S_2 state look essentially the same as for the S_1 state (36) and, therefore, it appears that the Mn site does not undergo a substantial structural reorganization during the S_1 to S_2 transition.

The EXAFS of Mn in photosystem II looks very much like that of a mixed-valence di- μ -oxo-bridged Mn dimer model compound (33,35). In particular, the Mn-Mn distance of 2.7 Å in photosystem II is characteristic of a di- μ -oxo-bridged structure. Recent EXAFS data have indicated that a second Mn-Mn distance of 3.3 Å may also be present (37-38). Although a clear picture of all of the Mn-Mn distances is not yet available, the EXAFS results are consistent with a structure in which two di- μ -oxo bridged Mn dimers are present in close proximity.

Of note is the apparent lack of chloride in the first coordination shell of Mn in either the S_1 or the S_2 state as revealed by EXAFS studies of Mn (35). This observation is of particular interest because chloride is required for optimal O_2 evolution rates (39) and has been proposed to act as a bridging ligand in a polynuclear Mn complex (40). Recent EPR studies, however, also suggest that chloride is not bound to Mn in the S_1 or S_2 state (41).

The energy of the X-ray absorption edge reflects the electron density about Mn which, in turn, reflects the oxidation state and ligation of Mn. The energy of the X-ray absorption edge of Mn in the S_1 state is in the range observed for Mn(III) model compounds (32,34). The X-ray absorption edge of Mn shifts to higher energy in the S_2 state and is in the range observed for Mn(III) and Mn(IV) model compounds (34). In light of the conclusion from the EXAFS studies that the coordination of Mn does not change substantially in the S_1 to S_2 transition (36), this result indicates that Mn is oxidized in the S_1 to S_2 transition. However, the shift in the Mn X-ray absorption edge is very small in the S_2 to S_3 transition, suggesting that Mn itself is not oxidized in this step (34,38).

These results seem to indicate that oxidation of Mn occurs in some, but not all, of the S-state transitions. This has led to proposals that redox-active centers other than Mn are involved in the storage of oxidizing equivalents during some of the S-state transitions. However, the energy of the Mn X-ray absorption edge reflects electron density about Mn and not directly the oxidation state. It is possible that the changes in the energy of the Mn X-ray absorption edge could be accounted for by a single oxidation of a Mn ion in both the S_1 to S_2 and S_2 to S_3 transitions if there is a change in ligation of the Mn ions in the S_2 to S_3 transition. Indeed, there is evidence that the substrate water coordinates to the Mn complex in the S_3 state (for a discussion see 27). The coordination of a Lewis base, such as water, to the Mn complex in the S_3 state would be expected to cause the shift of the Mn X-ray absorption edge in the S_2 to S_3 transition to be small even though the Mn complex is oxidized by one electron.

Ultraviolet Absorption Studies of the Manganese Complex

Flash-induced UV-difference spectral data indicate that a chromophore associated with the S states can be monitored in the 300-350 nm range (42-46). The difficulty with these measurements is that several other components in photosystem II also exhibit spectral changes in this region of the spectrum. After correcting for the absorbance changes due to redox changes of Q_A , Q_B (or an exogenous electron acceptor), and Z in photosystem II, Dekker et al. (42) found that the absorbance changes associated with the S_0 to S_1 , S_1 to S_2 , and S_2 to S_3 transitions were all equivalent and resembled the difference in absorbance between a Mn(III) and a Mn(IV)-gluconate model complex. Dekker et al. (42) concluded that one Mn(III) is oxidized to Mn(IV) in each of the first three S-state transitions. More recent work has considerably complicated this interpretation (43-46). It now seems probable that the absorbance changes are not all the same for the different S-state transitions. The most recent UV-spectral data are consistent with a single oxidation of Mn in each of the S-state transitions (45-46), although the assignment of the UV-difference spectra to the oxidation of Mn(III) to Mn(IV) is not clear because the spectral changes for the oxidation of Mn(II) to Mn(III) may be similar (47).

Structure of the Manganese Complex

The Mn-Mn distance of 2.7 Å determined by EXAFS is diagnostic of a di- μ -oxo-bridged Mn dimer in photosystem II (33,35). However, one could imagine a number of arrangements of the four Mn ions in photosystem II which contain a di- μ -oxo-bridged structure. Moreover, the observation of two different Mn-Mn distances by EXAFS, could only be accounted for by one of the following three arrangements of Mn: a Mn trimer plus one isolated (more than 3.3 Å away) Mn mononuclear center, two isolated inequivalent Mn dimers, or a Mn tetramer.

In order to distinguish between these possibilities, one must consider the EPR properties of the S_2 and S_3 states. Measurements have been made of the temperature dependence of the S_2 -state multiline (24,48-49) and $g = 4.1$ (24) EPR signals in order to

determine whether the EPR signals arise from the ground state or from a thermally-populated state. The S_2 -state $g = 4.1$ EPR signal exhibits Curie-law behavior characteristic of an EPR transition from a ground state or from a system in the high-temperature limit (24). It seems probable that the $g = 4.1$ EPR signal arises from a ground $S = 3/2$ state of a Mn species. The S_2 -state multiline EPR signal has been assigned to either a ground or low-lying $S = 1/2$ state of a multinuclear mixed-valence Mn species (24,48-49); and the S_3 state does not exhibit an EPR signal. These assignments severely restrict the possible arrangements of Mn in photosystem II and also provide important information on the structure of the Mn complex.

On the basis of a similarity of the ^{55}Mn nuclear hyperfine couplings in the S_2 -state multiline EPR signal with those of EPR signals from Mn dimer model complexes, it has been suggested that the S_2 -state multiline EPR signal arises from the $S = 1/2$ state of an antiferromagnetically exchange coupled mixed-valence Mn dimer (20,26). This assignment has led to proposals of a variety of models in which a Mn dimer is the catalytic site for water oxidation. Therefore, consider the magnetic properties of a binuclear mixed-valence Mn complex. A number of inorganic mixed-valence Mn dimers have been synthesized and their structures and magnetic properties have been determined (50-52). The unpaired electrons on each Mn ion are correlated through exchange interactions that arise from either direct orbital overlap or orbital overlap that is mediated by the bridging ligands (53). For a binuclear Mn complex, a single isotropic exchange coupling constant, J , usually is sufficient to account for the magnetic properties. Using the Heisenberg exchange Hamiltonian (Equation 2) one obtains the energy levels (Equation 3) for a pair of Mn ions with electron spins of S_A and S_B , respectively.

$$\hat{H}_{ex} = J \hat{S}_A \cdot \hat{S}_B = \frac{1}{2} J (\hat{S}^2 - \hat{S}_A^2 - \hat{S}_B^2) \quad (2)$$

$$\text{Energy} = E = \frac{1}{2} J [S(S+1) - S_A(S_A+1) - S_B(S_B+1)] \quad (3)$$

Figure 2 depicts the energies of the spin states that arise from either antiferromagnetic or ferromagnetic exchange coupling of a Mn(III)-Mn(IV) dimer. For di- μ -oxo-bridged Mn(III)-Mn(IV) model complexes, the exchange coupling is typically antiferromagnetic, in which case the ground state has $S = 1/2$. Observation of a Curie-law behavior for the temperature dependence of the S_2 -state multiline EPR signal is also consistent with this EPR signal arising from the ground $S = 1/2$ state of an antiferromagnetically exchange-coupled Mn dimer (48).

The assignment of the S_2 -state multiline EPR signal to a Mn dimer must be considered in light of the assignment of the S_2 -state $g = 4.1$ EPR signal to a ground $S = 3/2$ state of a Mn species. From Figure 2, it is apparent that the S_2 -state $g = 4.1$ EPR signal does not arise from a magnetically-isolated mixed-valence Mn dimer. Several assignments of the S_2 -state $g = 4.1$ EPR signal have been proposed. The $g = 4.1$ EPR signal could arise from a mononuclear high-spin Mn(IV) which has $S = 3/2$ (26), from an $S = 3/2$ state of an exchange coupled trinuclear Mn complex (54), or from an $S = 3/2$ state of an exchange coupled tetranuclear Mn complex (24). All of

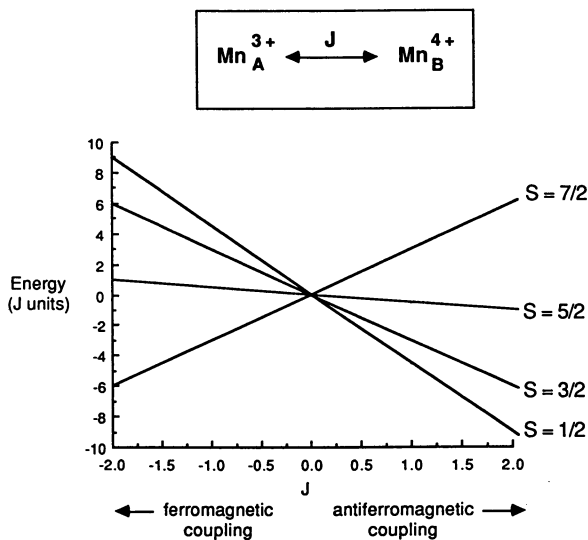


Figure 2: Energy levels given by Equation 3 for an exchange coupled Mn(III)-Mn(IV) dimer.

these possibilities are supported by observations of EPR signals near $g = 4$ from well-characterized Mn model complexes.

If we return to the possible arrangements of Mn in photosystem II that are consistent with the EXAFS data, one can rule out the possibility that the Mn ions are arranged as two isolated inequivalent Mn dimers because this arrangement cannot account for the S_2 -state $g = 4.1$ EPR signal. This leaves two possible arrangements of the Mn ions: a Mn trimer plus a mononuclear Mn center, or a Mn tetramer. Consequently, one should look for an assignment for the S_2 -state multiline EPR signal from either a mixed-valence Mn trimer or tetramer rather than from a mixed-valence Mn dimer.

The ^{55}Mn nuclear hyperfine couplings for the S_2 -state multiline EPR signal strongly resemble those for mixed-valence Mn dimers. However, the ^{55}Mn nuclear hyperfine couplings for a Mn trimer or tetramer depend on the projection of each Mn ion's nuclear hyperfine coupling tensor on the total spin of the system. It has been shown that only two Mn ions will contribute significantly to the ^{55}Mn nuclear hyperfine couplings for a Mn tetramer if the tetramer is composed of two antiferromagnetically exchange coupled Mn dimers that are ferromagnetically exchange coupled (24). Consequently, it is not always possible to determine the number of Mn ions in a multinuclear Mn complex simply on the basis of the ^{55}Mn nuclear hyperfine couplings.

Consider next, the magnetic properties of a Mn tetramer. For a Mn tetramer, six isotropic exchange couplings are required to model the magnetic properties. In order to reduce the number of variables in a simulation of the magnetic properties, it has been assumed that some of the exchange couplings are equal (24). Consider a Mn tetramer composed of two Mn dimers in which the interdimer Mn exchange couplings are all equivalent (Figure 3). In this case, the number of exchange coupling constants is reduced to three and the energies can be solved analytically (55). Call one pair of Mn ions A and B and the second pair of Mn ions C and D. The exchange Hamiltonian is given in Equation 4.

$$\hat{H}_{\text{ex}} = J_{AB} \hat{S}_A \cdot \hat{S}_B + J_{CD} \hat{S}_C \cdot \hat{S}_D + J(\hat{S}_A \cdot \hat{S}_C + \hat{S}_A \cdot \hat{S}_D + \hat{S}_B \cdot \hat{S}_C + \hat{S}_B \cdot \hat{S}_D) \quad (4)$$

Making the substitution of $\hat{S}' = \hat{S}_A + \hat{S}_B$ and $\hat{S}^* = \hat{S}_C + \hat{S}_D$ gives:

$$\hat{H}_{\text{ex}} = \frac{1}{2}J_{AB}(\hat{S}'^2 - \hat{S}_A^2 - \hat{S}_B^2) + \frac{1}{2}J_{CD}(\hat{S}^{*2} - \hat{S}_C^2 - \hat{S}_D^2) + \frac{1}{2}J(\hat{S}^2 - \hat{S}'^2 - \hat{S}^{*2}) \quad (5)$$

The energies for this system are given in Equation 6.

$$E(S, S', S^*) = \frac{1}{2}J_{AB} [S'(S' + 1) - S_A(S_A + 1) - S_B(S_B + 1)] + \frac{1}{2}J_{CD} [S^*(S^* + 1) - S_C(S_C + 1) - S_D(S_D + 1)] + \frac{1}{2}J [S(S + 1) - S'(S' + 1) - S^*(S^* + 1)] \quad (6)$$

Three possible combinations of Mn oxidation states are compatible with the EPR data from the S_2 state: Mn(II)-Mn(III)_3 , $\text{Mn(III)}_3\text{-Mn(IV)}$, and Mn(III)-Mn(IV)_3 (56-57). The most probable oxidation state is Mn(III)-Mn(IV)_3 (57). For a Mn(III)-Mn(IV)_3 complex the energy expression reduces to that shown in Equation 7.

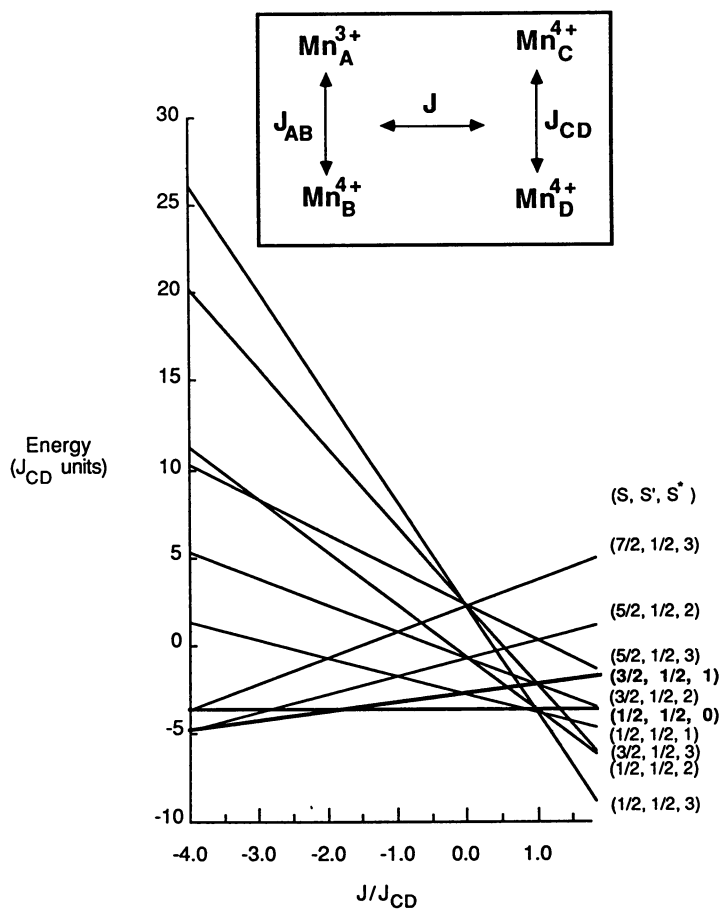


Figure 3: Lowest energy levels given by Equation 7 for an exchange coupled $Mn(III)-Mn(IV)_3$ tetramer in the limit where J_{AB} is large and positive. The $(S, S', S^*) = (3/2, 1/2, 1)$ and $(1/2, 1/2, 0)$ states, shown in bold, are proposed to give rise to the S_2 -state $g = 4.1$ and multiline EPR signals, respectively.

$$\begin{aligned}
 E(S, S', S^*) = & \frac{1}{2} J_{AB} [S'(S' + 1) - 39/4] \\
 & + \frac{1}{2} J_{CD} [S^*(S^* + 1) - 15/2] \\
 & + \frac{1}{2} J [S(S + 1) - S'(S' + 1) - S^*(S^* + 1)] \quad (7)
 \end{aligned}$$

Three criteria must be met for a Mn tetramer to account for the properties of the S_2 -state EPR signals. For one conformation of the Mn complex, the ground state should have $S = 3/2$ to account for the $g = 4.1$ EPR signal; for another conformation, the ground state or a low-lying excited state should have $S = 1/2$ to account for the multiline EPR signal; and the ^{55}Mn nuclear hyperfine interaction in the $S = 1/2$ state giving rise to the multiline EPR signal should be dominated by only two of the Mn ions. It has been shown (24) that this last criterion is satisfied for the $(S, S', S^*) = (1/2, 1/2, 0)$ state of a Mn tetramer (Figure 3).

If the exchange coupling between the Mn(III)-Mn(IV) dimer in a Mn tetramer, J_{AB} , is large and positive (antiferromagnetic coupling), and if J_{CD} is positive and J is negative, then the EPR properties of the S_2 state can be explained by a Mn tetramer model. Figure 3 gives the energy levels for a Mn tetramer when the exchange couplings, J and J_{CD} , are varied, in the limit when J_{AB} is large and positive. In order to produce a ground $S = 3/2$ state which could account for the S_2 -state $g = 4.1$ EPR signal, J_{CD} must be positive, and J must be negative; further, J/J_{CD} must lie between -2 and -4 . It is expected that the exchange couplings in the two conformations that give the S_2 -state $g = 4.1$ and multiline EPR signals, respectively, will be similar because these two conformations interconvert at 200 K or below, temperatures at which only minor structural changes are expected to occur. Note that the $(1/2, 1/2, 0)$ state, from which the S_2 -state multiline EPR signal could arise, is the first excited state when J/J_{CD} is between -2 and -3 and is the ground state when J/J_{CD} is between 1 and -2 . Consequently, no major changes in the exchange couplings are required in order to explain the conversion of the S_2 -state $g = 4.1$ EPR signal into the multiline EPR signal with a Mn tetramer model.

Further work will be needed to test whether or not a trimer/monomer arrangement of Mn can account for the magnetic properties of the S_2 state. However, it is clear that all of the magnetic properties of the S_2 state can be accounted for with a Mn tetramer. One conclusion that can be drawn is that both antiferromagnetic and ferromagnetic exchange couplings must be present simultaneously in order for a tetramer model to account for the magnetic properties of the Mn complex in the S_2 state. This unusual combination of exchange couplings has been previously observed for "cubane"-like complexes (58-59), and this analogy suggests that the tetrameric Mn complex may have a "cubane"-like structure in the S_2 state (24). An oxo-bridged "cubane"-like Mn tetrameric complex was proposed for the structure of the Mn complex in the S_2 state (24,57). A distortion of an oxo-bridged "cubane"-like Mn tetramer seems to best account for the arrangement of Mn ions as seen by both EXAFS and EPR in the S_2 state.

Mechanism of Water Oxidation

Many proposals have been made for the role of Mn in photosynthetic water oxidation (for reviews see 3-6). It is clear that Mn

functions both to accumulate the oxidizing equivalents produced during S-state advancement and also to bind water and catalyze its oxidation. The EXAFS and EPR data described in the previous sections are best accounted for by a tetrameric Mn complex with a distorted oxo-bridged "cubane"-like structure in the S_2 state. How might this site catalyze the water oxidation reaction?

The key step in the formation of an O_2 molecule is the activation of a bound water in order to form an O-O bond. This step is likely to be energetically the most demanding, and it is quite reasonable that the formation of the O-O bond does not occur until the most highly oxidized state of Mn is attained. An analogy can be drawn between photosynthetic water oxidation and the chemistry of cytochrome P450; in both cases a water molecule must be activated for reaction with a nucleophile. In cytochrome P450 model systems, oxidation of Fe or Mn to Fe(V) or Mn(V), respectively, is required to activate water to abstract a hydrogen atom from a hydrocarbon or to add to an olefin to form an epoxide (60). On this basis, a Mn(V) oxidation state may be needed to trigger the oxidation of water in photosystem II. The most probable oxidation state of Mn in the S_2 state is Mn(III)-Mn(IV)₃ (57). This oxidation state of the Mn complex in the S_2 state is also consistent with recent Mn X-ray absorption edge studies (38). Sequential one-electron oxidations of the Mn complex would then produce the S_4 state containing Mn(IV)₃-Mn(V).

A number of proposals for the mechanism of O_2 formation involve the generation of an O-O bond before the S_4 state is produced (reviewed in 6,61). These proposals seem less likely based on a consideration of the energetic requirements for water activation (62). There is also evidence from mass spectrometric studies of the isotopic composition of O_2 evolved from photosystem II that the water molecules that are oxidized to O_2 do not bind to the O_2 -evolving center, or that they exchange readily with bulk water, in the S_0 , S_1 , S_2 , and S_3 states (63). This result would be difficult to accommodate if the O-O bond is formed in one of the earlier S-state transitions.

A consideration of the evidence available on the natural system, as well as the coordination chemistry of Mn, led us to propose the model for water oxidation shown in Figure 4 (57). EPR spectral data obtained from the S_2 state are characteristic of a Mn₄O₄ "cubane"-like structure (24) and EXAFS studies of Mn indicate that the Mn site does not undergo a substantial structural change on going from S_1 to S_2 (36). Hence, the tetrameric Mn complex was proposed to exist in a Mn₄O₄ "cubane"-like structure in the lower oxidation states (S_0 to S_2). Studies of ammonia binding to the O_2 -evolving center show that the Mn complex in the lower oxidation states (S_0 and S_1) is inert to nucleophilic addition, whereas the higher oxidation states (S_2 and S_3) are reactive to nucleophilic addition of ammonia (28,64). The activation of the Mn complex for nucleophilic addition in the higher S states is accounted for in this model by the sequential oxidation of Mn without accommodation of the ligand environment. This leads to a progressive increase in electron deficiency of the Mn complex with a corresponding increase in reactivity of the Mn complex to nucleophilic addition with increasing S state. Upon reaching the S_3 state it was suggested that the Mn complex coordinates two O^{2-} or OH^- ions from water

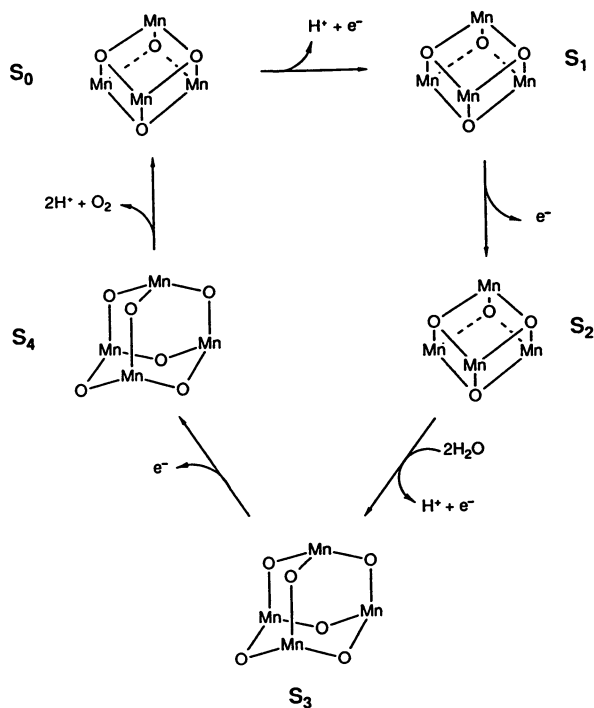


Figure 4: A proposed scheme for the structures of Mn associated with the S state transitions. In this scheme, O denotes either O^{2-} or OH^- ligands. Each Mn ion in the tetrameric complex is proposed to also be coordinated to the protein via three O or N ligands, as indicated by EXAFS studies of Mn in the S_1 state (33,35), although the protein-derived ligands are not shown.

molecules and undergoes a structural rearrangement to form a Mn_4O_6 "adamantane"-like structure. Further oxidation of the Mn complex generates the S_4 state which was proposed to be initially formed with a Mn_4O_6 structure. The electron withdrawal by high-valent Mn from the O ligands then triggers the formation of an O-O bond. A molecule of O_2 is released via reduction of the Mn complex and conversion of the μ_2 -oxo ligands into μ_3 -oxo ligands.

I have presented an overview of the current state-of-the-art in studies of the Mn complex in photosystem II. There are many unresolved questions and a clear picture of the structure and function of Mn in photosynthetic water oxidation is still not available. One useful approach to help determine the structure of the Mn complex in photosystem II involves the synthesis and characterization of Mn model complexes for comparison with the properties of the Mn complex in photosystem II. Recently, several tetrameric high-valent Mn-oxo complexes have been reported (see the chapter in this volume by G. Christou). Further characterization of existing and new high-valent tetrameric Mn-oxo model complexes, especially EPR and EXAFS measurements, will no doubt help clarify the present uncertain picture of the structure of the Mn complex in photosystem II.

Acknowledgments

I thank Warren Beck for help with the preparation of the figures and Warren Beck and Lynmarie Thompson for helpful comments on this manuscript. This work was supported by the National Institutes of Health (GM32715). G.W.B. is the recipient of a Camille and Henry Dreyfus Teacher/Scholar Award (1985-1990) and an Alfred P. Sloan Foundation Research Fellowship (1986-1988).

Literature Cited

1. Stallings, W.C.; Pattridge, K.A.; Strong, R.K.; Ludwig, M.L. *J. Biol. Chem.* **1984**, *259*, 10695-99.
2. Beyer, W.F., Jr.; Fridovich, I. *Biochemistry* **1985**, *24*, 6460-67.
3. Ames, J. *Biochim. Biophys. Acta* **1983**, *726*, 1-12.
4. Dismukes, G.C. *Photochem. Photobiol.* **1986**, *43*, 99-115.
5. Babcock, G.T. In *New Comprehensive Biochemistry: Photosynthesis*; Ames, J., Ed.; Elsevier: Amsterdam, 1987, pp. 125-58.
6. Brudvig, G.W. *J. Bioenerg. Biomemb.* **1987**, *19*, 91-104.
7. Pirson, A. Z. *Bot.* **1937**, *31*, 193-267.
8. Cheniae, G.M.; Martin, I.F. *Biochim. Biophys. Acta* **1970**, *197*, 219-39.
9. Cheniae, G.M. *Ann. Rev. Plant Physiol.* **1970**, *21*, 467-98.
10. Ghanotakis, D.F.; Yocum, C.F. *Photosyn. Res.* **1985**, *7*, 97-114.
11. Murata, N.; Miyao, M.; Omata, T.; Matsunami, H.; Kubawara, T. *Biochim. Biophys. Acta* **1984**, *765*, 363-69.
12. Joliot, P.; Barbieri, G.; Chabaud, R. *Photochem. Photobiol.* **1969**, *10*, 309-29.
13. Kok, B.; Forbush, B.; McGloin, M. *Photochem. Photobiol.* **1970**, *11*, 457-75.
14. Forbush, B.; Kok, B.; McGloin, M. *Photochem. Photobiol.* **1971**, *14*, 307-21.

15. Joliot, P.; Kok, B. In *Bioenergetics of Photosynthesis*; Govindjee, Ed.; Academic: New York, 1975, pp. 387-412.
16. Vermaas, W.F.J.; Renger, G.; Dohnt, G. *Biochim. Biophys. Acta* **1984**, *764*, 194-202.
17. Styring, S.; Rutherford, A.W. *Biochemistry* **1987**, *26*, 2401-05.
18. de Paula, J.C.; Innes, J.B.; Brudvig, G.W. *Biochemistry* **1985**, *24*, 8114-20.
19. Dismukes, G.C.; Siderer, Y. *FEBS Lett.* **1980**, *121*, 78-80.
20. Dismukes, G.C.; Siderer, Y. *Proc. Natl. Acad. Sci. USA* **1981**, *78*, 274-77.
21. Hansson, Ö.; Andréasson, L.-E. *Biochim. Biophys. Acta* **1982**, *679*, 261-68.
22. Casey, J.L.; Sauer, K. *Biochim. Biophys. Acta* **1984**, *767*, 21-28.
23. Zimmermann, J.-L.; Rutherford, A.W. *Biochim. Biophys. Acta* **1984**, *767*, 160-67.
24. de Paula, J.C.; Beck, W.F.; Brudvig, G.W. *J. Amer. Chem. Soc.* **1986**, *108*, 4002-09.
25. Zimmermann, J.-L.; Rutherford, A.W. *Biochemistry* **1986**, *25*, 4609-4615.
26. Hansson, Ö.; Aasa, R.; Vänngård, T. *Biophys. J.* **1987**, *51*, 825-32.
27. Beck, W.F. Ph.D. Thesis, Yale University, New Haven, 1988.
28. Beck, W.F.; de Paula, J.C.; Brudvig, G.W. *J. Amer. Chem. Soc.* **1986**, *108*, 4018-22.
29. Beck, W.F.; Brudvig, G.W. *Biochemistry* **1986**, *25*, 6479-86.
30. Hansson, Ö.; Andréasson, L.-E.; Vänngård, T. *FEBS Lett.* **1986**, *195*, 151-54.
31. Andréasson, L.-E.; Hansson, Ö. In *Progress in Photosynthesis Research* vol. 1; Biggins, J., Ed.; Nijhoff: Dordrecht, 1987, pp. 503-10.
32. Kirby, J.A.; Goodin, D.B.; Wydrzynski, T.; Robertson, A.S.; Klein, M.P. *J. Amer. Chem. Soc.* **1981**, *103*, 5537-42.
33. Kirby, J.A.; Robertson, A.S.; Smith, J.P.; Thompson, A.C.; Cooper, S.R.; Klein, M.P. *J. Amer. Chem. Soc.* **1981**, *103*, 5529-37.
34. Goodin, D.B.; Yachandra, V.K.; Britt, R.D.; Sauer, K.; Klein, M.P. *Biochim. Biophys. Acta* **1984**, *767*, 209-16.
35. Yachandra, V.K.; Guiles, R.D.; McDermott, A.E.; Britt, R.D.; Dexheimer, S.L.; Sauer, K.; Klein, M.P. *Biochim. Biophys. Acta* **1986**, *850*, 324-32.
36. Yachandra, V.K.; Guiles, R.D.; McDermott, A.E.; Cole, J.L.; Britt, R.D.; Dexheimer, S.L.; Sauer, K.; Klein, M. P. *Biochemistry* **1987**, *26*, 5974-5981.
37. George, G.N.; Prince, R.C.; Cramer, S.P. In *Stanford Synchrotron Radiation Laboratory Users Meeting Report* 1987.
38. Guiles, R.D.; Yachandra, V.K.; McDermott, A.E.; Britt, R.D.; Dexheimer, S.L.; Sauer, K.; Klein, M.P. In *Progress in Photosynthesis Research* vol. 1; Biggins, J., Ed.; Nijhoff: Dordrecht, 1987, pp. 561-64.
39. Kelley, P.; Izawa, S. *Biochim. Biophys. Acta* **1978**, *502*, 198-210.
40. Sandusky, P.O.; Yocum, C.F. *FEBS Lett.* **1983**, *162*, 339-43.
41. Yachandra, V.K.; Guiles, R.D.; Sauer, K.; Klein, M.P. *Biochim. Biophys. Acta* **1986**, *850*, 333-42.

42. Dekker, J.P.; van Gorkom, H.J.; Wensink, J.; Ouwehand, L. *Biochim. Biophys. Acta* **1984**, *767*, 1-9.
43. Laverne, J. *Photochem. Photobiol.* **1986**, *43*, 311-17.
44. Renger, G.; Hanssum, B.; Weiss, W. In *Progress in Photosynthesis Research* vol. 1; Biggins, J., Ed.; Nijhoff: Dordrecht, 1987, pp. 541-44.
45. Saygin, Ö.; Witt, H.T. *Biochim. Biophys. Acta* **1987**, *893*, 452-69.
46. Laverne, J. *Biochim. Biophys. Acta* **1987**, *894*, 91-107.
47. Vincent, J.B.; Christou, G. *FEBS Lett.* **1986**, *207*, 250-52.
48. Aasa, R.; Andréasson, L.-E.; Lagenfelt, G.; Vänngård, T. *FEBS Lett.* **1987**, *221*, 245-48.
49. de Paula, J.C.; Beck, W.F.; Miller, A.-F.; Wilson, R.B.; Brudvig, G.W. *J. Chem. Soc., Faraday Trans. 1* **1987**, *83*, 3635-51.
50. Cooper, S.R.; Dismukes, G.C.; Klein, M.P.; Calvin, M.C. *J. Amer. Chem. Soc.* **1978**, *100*, 7248-52.
51. Wieghardt, K.; Bossek, U.; Ventur, D.; Weiss, J. *J. Chem. Soc., Chem. Commun.* **1985**, 347-49.
52. Sheats, J.E.; Czernuszewicz, R.S.; Dismukes, G.C.; Rheingold, A.L.; Petroleas, V.; Stubbe, J.; Armstrong, W.H.; Beer, R.H.; Lippard, S.J. *J. Amer. Chem. Soc.* **1987**, *109*, 1435-44.
53. Cairns, C.J.; Busch, D.H. *Coord. Chem. Rev.* **1986**, *69*, 1-55.
54. Pecoraro, V.L.; Kessissoglou, D.P.; Li, X.; Butler, W.M. In *Progress in Photosynthesis Research* vol. 1; Biggins, J., Ed.; Nijhoff: Dordrecht, 1987, pp. 725-28.
55. Sinn, E. *Coord. Chem. Rev.* **1970**, *5*, 313-347.
56. Dismukes, G.C.; Ferris, K.; Watnick, P. *Photobiochem. Photobiophys.* **1982**, *3*, 243-256.
57. Brudvig, G.W.; Crabtree, R.H. *Proc. Natl. Acad. Sci. USA* **1986**, *83*, 4586-88.
58. Noodleman, L.; Norman, J.G., Jr.; Osborne, J.H.; Aizman, A.; Case, D.A. *J. Amer. Chem. Soc.* **1985**, *107*, 3418-26.
59. Haase, W.; Walz, L.; Nepveu, F. In *The Coordination Chemistry of Metalloenzymes*; Bertini, I., Drago, R.S., Luchinat, C., Eds.; D. Reidel Publishing Company: Holland, 1983, pp. 229-34.
60. Sheldon, R.A.; Kochi, J.K. *Metal Catalyzed Oxidations of Organic Compounds*; Academic: New York, 1981.
61. Renger, G.; Govindjee *Photosynth. Res.* **1985**, *6*, 33-55.
62. Brudvig, G.W.; de Paula, J.C. In *Progress in Photosynthesis Research* vol. 1; Biggins, J., Ed.; Nijhoff: Dordrecht, 1987, pp. 491-98.
63. Radmer, R.; Ollinger, O. *FEBS Lett.* **1986**, *195*, 285-89.
64. Velthuys, B.R. *Biochim. Biophys. Acta* **1975**, *396*, 392-401.

RECEIVED February 3, 1988